

Article

# Impact of periodicity and stochastic impact on COVID-19 pandemic: A mathematical model

Kalyan Das<sup>1</sup>, Ranjith Kumar<sup>2</sup>, Prasenjit Das<sup>3</sup>

<sup>1</sup>Department of Basic and Applied Sciences, National Institute of Food Technology, Entrepreneurship and Management, HSIIDC Industrial Estate, Kundli, Haryana, India

<sup>2</sup>Anurag University, Hyderabad, Telangana, India

<sup>3</sup>Srichanda M.N.M. Institution, South 24 Parganas-743375, India

E-mail: daskalyan27@gmail.com, ranjithreddy1982@gmail.com, pdas1970@gmail.com

Received 11 May 2022; Accepted 15 June 2022; Published online 20 July 2022; Published 1 September 2022



## Abstract

We analyzed the features of the COVID-19 outbreak with temporal delay and stochastic influence using the SIRS epidemic model in this study. We investigate the local stability of each equilibrium point in terms of basic reproduction numbers. Hopf bifurcation is detected in the system, and a time delay is inserted in the transmission terms to represent the virus's incubation period. The spread of the novel COVID-19 strain to humans is influenced by environmental conditions such as mugginess, precipitation, and temperature. To explore the impact of environmental oscillations on the coronavirus, we employ white noise perturbations in the system. Finally, we examine the mathematical reenactments using MATLAB.

**Keywords** COVID-19; stability; Hopf-bifurcation; stochasticity; white noise.

Network Biology  
ISSN 2220-8879  
URL: <http://www.iaees.org/publications/journals/nb/online-version.asp>  
RSS: <http://www.iaees.org/publications/journals/nb/rss.xml>  
E-mail: [networkbiology@iaees.org](mailto:networkbiology@iaees.org)  
Editor-in-Chief: WenJun Zhang  
Publisher: International Academy of Ecology and Environmental Sciences

## 1 Introduction

COVID-19, a fast spreading coronavirus disease, has become a global emergency. This contagious disease is rapidly spreading, endangering the lives of many people. As a result, timely interventions and thorough examinations are likely to keep the disease at bay in networks (Hui et al., 2020). The COVID-19 pollution manifests itself as COVID-19. Hacking, fever, tiredness, loose bowels, and windedness are all symptoms. COVID-19 typically causes pneumonia and, in severe cases, death (WHO, 2020). COVID-19 has a hatching time of 3–14 days or longer, according to the essential investigations (WHO-China, 2020). Due to various applications of fractional calculus, stochastic modelling and bifurcation analysis (Xu et al., 2017, 2019; Xu et al., 2019a; Xu et al., 2020b; Abdon, 2017, 2018, 2020; Shah et al., 2020), several analysts analyzed this COVID-19 in many models in full and partial requests (Nesteruk, 2020; Okhueuse, 2020; Zhou et al., 2020; Bogoch et al., 2020; Ji et al., 2020; Li et al., 2020; Yousaf et al., 2020; Ud Din et al., 2020; Cakan, 2020; Abdo et al., 2020; Khan et al., 2020; Zeb et al., 2020). A few creators considered stochastic models by giving repetitive noises for the more practical models (Tornatore et al., 2005). To be honest, stochastic nuisance

elements such as precipitation, total moisture, and temperature have a major impact on the contamination capacity of a wide range of infectious diseases in humans. Thinking about this allows us to bring irregularity into deterministic natural models in order to uncover the impact of ecological changeability, whether it's ecological vacillations in borders or arbitrary commotion in differential frameworks (Yang et al., 2013; Lahrouz et al., 2014; Liu et al., 2018; Zhao et al., 2019; Wei et al., 2020). Several authors (Bahar et al., 2004; Mao et al., 2003, 2005) have focused on stochastic population elements bothered by repeating sound in general (Brownian movement).

Using a SIRS epidemic model, we analyzed the dynamics of COVID-19 infection among groups in this study. The incubation period of an infection is referred to as a time delay in the transmission terminology (Zhang et al., 2020). The effects of environmental variations and parameter variability are also shown using environmental variations and parameter variability. A synopsis of the paper is as follows: We present a stochastic SIRS model with a time delay in Section 1. Section 2 looked into the stability of each equilibrium point. In Section 3, the model's existence of Hopf bifurcation was investigated. We looked at the stochastic stability of the recommended model in Section 4. Several numerical examples are included in Section 5. Finally, there are some final remarks in Section 6.

Let us assume that a human population is divided into three classes: Susceptible, Infected and Recovered (Zhang et al., 2020). The sizes of these groups are represented by  $S(t)$ ,  $I(t)$  and  $R(t)$  respectively. All recruitment is into the susceptible class, and occurs at a constant rate  $b$ . Let  $\mu$  is natural death rate and  $d$  is disease induced death rate. Let us assume the susceptible is infected through virus and soon certain individuals became infected. Here, we use nonlinear saturation incidence rate  $\beta SI/a + \alpha I$  where  $\beta I$  measures the infection force of the disease and  $1/a + \alpha I$  measures the inhabitation effect/crowding effect.  $a$  and  $\alpha$  are certain constants. Considering  $r$  as recovery rate of infected human population through medication and quarantine and  $\eta$  as rate of transfer from Recovered to susceptible class we formulate the following model (Fig. 1):

$$\begin{aligned} \dot{S} &= b - \frac{\beta SI}{a + \alpha I} - \mu S + \eta R \\ \dot{I} &= \frac{\beta SI}{a + \alpha I} - (r + d)I \\ \dot{R} &= rI - (\eta + \mu)R \end{aligned} \tag{1}$$

where  $S(0) > 0, I(0) > 0, R(0) > 0$ .

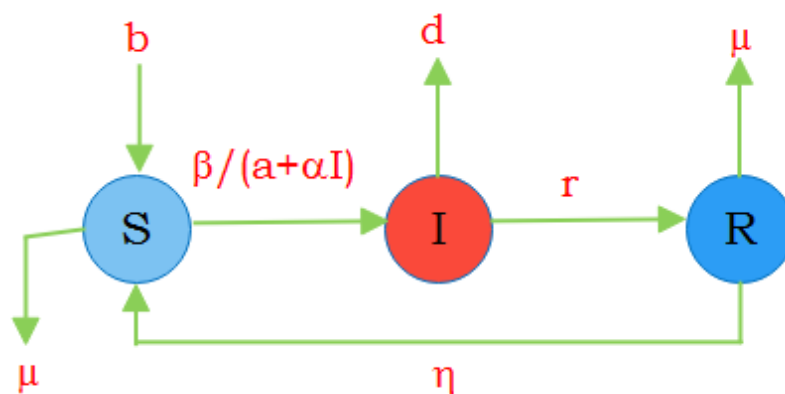


Fig. 1 Flow chart of SIRS model (1).

## 2 Equilibrium Points and Their Stability Analysis

The equilibrium points of the system (1) are given by i) disease free equilibrium point or corona virus free equilibrium point  $E_0\left(\frac{b}{\mu}, 0, 0\right)$  and ii) Endemic equilibrium point  $E_0\left(S^*, I^*, R^*\right)$ , where

$$S^* = \frac{1}{\beta}(r+d)(a + \alpha I^*),$$

$$I^* = \frac{[b\beta - \mu a(r+d)](\eta + \mu)}{\mu(r+d)[\beta + \alpha(\eta + \mu)] + \eta\beta d} \text{ and } \frac{rI^*}{\eta + \mu}. \text{ Clearly endemic equilibrium point exist when } R_0 > 1,$$

$$\text{where the basic reproduction number } R_0 = \frac{b\beta}{\mu a(r+d)}. \quad (2)$$

The system (1)'s asymptotic stability is explored further down.

### 2.1 At the disease-free equilibrium point, (1) is stable

**Theorem 1:** The Disease free equilibrium is asymptotically stable if  $R_0 < 1$ .

**Proof:** The system's Jacobian matrix at disease-free equilibrium is defined as

$$J_0 = \begin{bmatrix} -\mu & -\frac{b\beta}{a\mu} & \eta \\ 0 & \frac{b\beta}{a\mu} - (r+d) & 0 \\ 0 & r & -(\eta + \mu) \end{bmatrix} \quad (3)$$

The above matrix's characteristic equation is

$$-(\mu + \lambda) \left[ \left( \frac{b\beta}{a\mu} - (r+d) - \lambda \right) (-(\eta + \mu) - \lambda) \right] = 0$$

$$\text{Thus the eigenvalues are } \lambda_1 = -\mu, \lambda_2 = -(\eta + \mu), \lambda_3 = \frac{b\beta}{a\mu} - (r+d)$$

Here, first two eigenvalues are negative and third eigenvalue  $\lambda_3$  is negative if  $\frac{b\beta}{a\mu(r+d)} < 1$  i.e.,  $R_0 < 1$ .

As a result, the asymptotically stable disease-free equilibrium point exists.

### 2.2 Stability of (1) at endemic equilibrium point

**Theorem 2:** The Endemic equilibrium is asymptotically stable if  $R_0 > 1$ .

**Proof:** At the disease-free equilibrium point, the Jacobian matrix of the system is defined as

$$J_1 = \begin{bmatrix} -\frac{\beta I^*}{a + \alpha I^*} - \mu & -\frac{a\beta S^*}{(a + \alpha I^*)^2} & \eta \\ \frac{\beta I^*}{a + \alpha I^*} & -\frac{\alpha\beta S^* I^*}{(a + \alpha I^*)^2} & 0 \\ 0 & r & -(\eta + \mu) \end{bmatrix} \tag{4}$$

The above matrix's characteristic equation is

$$\lambda^3 + L_1\lambda^2 + L_2\lambda + L_3 = 0$$

Where  $L_1 = \frac{\beta I^*}{a + \alpha I^*} + \frac{a\beta S^*}{(a + \alpha I^*)^2} + (\eta + \mu) + \mu$

$$L_2 = \frac{a\beta^2 S^* I^{*2}}{(a + \alpha I^*)^3} + \frac{\alpha\beta S^* I^* (2\mu + \eta)}{(a + \alpha I^*)^2} + \frac{\beta I^* (\eta + \mu)}{a + \alpha I^*} + \mu(\eta + \mu) + \frac{a\beta^2 S^* I^*}{(a + \alpha I^*)^3}$$

$$L_3 = -\frac{r\eta\beta I^*}{a + \alpha I^*} + (\eta + \mu) \left[ \frac{\alpha\beta^2 S^* I^{*2}}{(a + \alpha I^*)^3} + \frac{\mu\alpha\beta S^* I^*}{(a + \alpha I^*)^2} + \frac{a\beta^2 S^* I^*}{(a + \alpha I^*)^3} \right]$$

Clearly  $L_1, L_2 > 0$  and simplifying  $L_3$  then

$$L_3 = \frac{1}{(a + \alpha I^*)^3} \left[ (a + \alpha I^*)^2 I^* (r\beta\mu + d\beta\eta + d\beta\mu + (\eta + \mu)\mu\alpha(r + d)) \right]$$

Therefore,  $L_1, L_2$  and  $L_3 > 0$  if  $R_0 > 1$ . To show the stability of endemic equilibrium next we have to show

that  $L_1L_2 - L_3 > 0$ .

$$L_1L_2 - L_3 = \left[ \frac{\beta I^*}{a + \alpha I^*} + \frac{a\beta S^*}{(a + \alpha I^*)^2} + \mu \right]$$

Where 
$$\left[ \frac{a\beta^2 S^* I^{*2}}{(a + \alpha I^*)^3} + \frac{\alpha\beta S^* I^* (2\mu + \eta)}{(a + \alpha I^*)^2} + \frac{\beta I^* (\eta + \mu)}{a + \alpha I^*} + \mu(\eta + \mu) + \frac{a\beta^2 S^* I^*}{(a + \alpha I^*)^3} \right]$$

$$+ (\eta + \mu) \left[ \frac{\alpha\beta S^* I^* (\mu + \eta)}{(a + \alpha I^*)^2} + \frac{\beta I^* (\eta + \mu)}{a + \alpha I^*} + \mu(\eta + \mu) \right] + \frac{r\eta\beta I^*}{a + \alpha I^*} > 0$$

Therefore  $L_1L_2 - L_3 > 0$  if  $R_0 > 1$ . Hence by Routh-Hurwitz criteria endemic equilibrium point is

asymptotically stable if  $R_0 > 1$ .

### 3 Stability Analysis with Time Delay

To replicate the incubation period of 3–14 days, we use a discrete time delay in the SIRS model (Grifoni et al., 2020). In transmission terms, time-delay  $\tau > 0$  refers to the time between the commencement of the disease and the onset of the side effects, as well as the time between the onset of the disease and the onset of the side effects. According to current research, early verified COVID-19 cases have an incubation time of about 5.5 days, which is similar to SARS-CoV. When time-delay is present in the model, intermittent setups are common for various time-delay values  $\tau$  (Bocharov et al., 2000). As a result, the following is a new formulation of the model:

$$\begin{aligned}\dot{S} &= b - \frac{\beta SI(t-\tau)}{a + \alpha I(t-\tau)} - \mu S + \eta R \\ \dot{I} &= \frac{\beta SI(t-\tau)}{a + \alpha I(t-\tau)} - (r + d)I \\ \dot{R} &= rI - (\eta + \mu)R\end{aligned}\tag{5}$$

We now discuss Hopf bifurcation aspects into the system5.

**Theorem 3:** Hopf bifurcation occurs in system (5) at the endemic equilibrium point when  $\tau = \tau_0$ .

**Proof:** The above system's Jacobian matrix is

$$J^* = \begin{bmatrix} -\frac{\beta I^*}{a + \alpha I^*} - \mu & -\frac{a\beta S^* e^{-\lambda\tau}}{(a + \alpha I^*)^2} & \eta \\ \frac{\beta I^*}{a + \alpha I^*} & -\frac{\alpha\beta S^* I^* e^{-\lambda\tau}}{(a + \alpha I^*)^2} - (r + d) & 0 \\ 0 & r & -(\eta + \mu) \end{bmatrix}$$

The Jacobian matrix's characteristic equation is as follows:

$$\lambda^3 + H_1\lambda^2 + H_2\lambda + H_3 + e^{-\lambda\tau}(M_1\lambda^2 + M_2\lambda + M_3) = 0\tag{6}$$

$$\text{Where } H_1 = \frac{\beta I^*}{a + \alpha I^*} + (\eta + \mu) + \mu + (r + d)$$

$$H_2 = (r + d)(\eta + \mu) + \frac{\beta I^*}{(a + \alpha I^*)}(r + d) + \frac{\beta I^*}{a + \alpha I^*}(\eta + \mu) + \mu(\eta + \mu) + \mu(r + d)$$

$$H_3 = \mu(r + d)(\eta + \mu) + \frac{\beta I^*}{(a + \alpha I^*)}(r + d)(\eta + \mu) - \frac{\beta I^*}{a + \alpha I^*}r\eta$$

$$M_1 = -\frac{a\beta S^*}{(a + \alpha I^*)^2}, M_2 = -\frac{a\beta S^*(\eta + \mu)}{(a + \alpha I^*)^2} - \frac{\mu a\beta S^*}{(a + \alpha I^*)^2}, M_3 = -\frac{\mu a\beta S^*(\eta + \mu)}{(a + \alpha I^*)^2}$$

If a latent roots of the equation (6) crosses the imaginary axis then instability occurs for a critical value of

$\tau > 0$ . We have from corollary 4 in (Ruan and Wei, 2003).

Substituting  $\lambda = i\omega$  into (6) gives

$$-H_1\omega^2 + H_3 + (M_3 - M_1\omega^2)\cos \omega\tau + M_2\omega \sin \omega\tau + i(-\omega^3 + H_2\omega + M_2\omega \cos \omega\tau + (M_1\omega^2 - M_3)\sin \omega\tau) = 0 \tag{7}$$

Comparing real and imaginary parts, we obtain

$$(M_3 - M_1\omega^2)\cos \omega\tau + M_2\omega \sin \omega\tau = H_1\omega^2 - H_3 \tag{8}$$

$$M_2\omega \cos \omega\tau - (M_3 - M_1\omega^2)\sin \omega\tau = \omega^3 - H_2\omega$$

Squaring and adding above two equations

$$\omega^6 + (H_1^2 - 2H_2 - M_1^2)\omega^4 + (H_2^2 - 2H_1H_3 + 2M_1M_3 - M_2^2)\omega^2 + (H_3^2 - M_3^2) = 0 \tag{9}$$

Let  $z = \omega^2$  then (9) becomes

$$z^3 + C_1z^2 + C_2z + C_3 = 0 \tag{10}$$

Where  $C_1 = H_1^2 - 2H_2 - M_1^2$ ;  $C_2 = H_2^2 - 2H_1H_3 + 2M_1M_3 - M_2^2$ ;  $C_3 = H_3^2 - M_3^2$ ;

Let  $\phi(z) = z^3 + C_1z^2 + C_2z + C_3$  and  $\lim_{z \rightarrow \infty} \phi(z) = +\infty$ ,  $C_3 < 0$ , equation (10) can have at least one positive root. Without loss of generality, assume that equation (10) has all roots as positive. Therefore, the three positive roots of (9) are given by

$$\omega_1 = \sqrt{z_1}, \omega_2 = \sqrt{z_2}, \omega_3 = \sqrt{z_3}$$

From (8), we obtain  $\tau_0$ , which is the minimum of  $\tau_k, k = 1, 2, 3$  and from this we get the roots  $\pm i\omega_k$  of the equation (6).

The next step is to prove that at endemic equilibrium, the system (5) goes through Hopf bifurcation when  $\tau = \tau_0$ .

Differentiating (6) with respect to  $\tau$ , we get

$$\left(\frac{d\lambda}{d\tau}\right)^{-1} = \frac{3\lambda^2 + 2H_1\lambda^2 + H_2}{(M_1\lambda^2 + M_2\lambda + M_3)\lambda e^{-\lambda\tau}} + \frac{2M_1\lambda + M_2}{(M_1\lambda^2 + M_2\lambda + M_3)\lambda} - \frac{\tau}{\lambda}$$

Substituting  $\lambda = i\omega_0$  and from (8), we get

$$\text{Re}\left(\frac{d\lambda}{d\tau}\right)^{-1}\bigg|_{\lambda=i\omega_0} = \frac{3\omega_0^4 - 2(2H_2 - H_1^2 + M_1^2)\omega_0^2 + H_2^2 - M_2^2 + 2M_1M_3}{\psi_1^2 + \psi_2^2}$$

Where  $\psi_1^2 = (M_3 - M_1\omega_0^2)\sin \omega_0\tau - M_2\omega_0 \cos \omega_0\tau$ ;  $\psi_2^2 = M_2\omega_0 \sin \omega_0\tau + (M_3 - M_1\omega_0^2)\cos \omega_0\tau$

then  $\text{Re}\left(\frac{d\lambda}{d\tau}\right)^{-1}\bigg|_{\lambda=i\omega_0} > 0$  if  $(2H_2 - H_1^2 + M_1^2) < 3(H_2^2 - M_2^2 + 2M_1M_3)$

Hence the system (5) go through the Hopf bifurcation at endemic equilibrium when  $\tau = \tau_0$  (Hale, 1977, and Kuang, 1993).

#### 4 Stochastic Analysis with External Driving Force

In this part, we use white noise theory to present the system's external disturbances (1). At the positive equilibrium point, these findings are discussed. To discuss the stability of the stochastic system, we consider the linearized model with the perturbations  $x_1, x_2$  and  $x_3$ . The system's stochastic stability was determined using mean-square fluctuations. The stochastic perturbed system is given

$$\frac{dS(t)}{dt} = \left[ b - \frac{\beta SI}{a + \alpha I} - \mu S + \eta R \right] dt + p_1 \xi_1(t) \quad (11)$$

$$\frac{dI(t)}{dt} = \left[ \frac{\beta SI}{a + \alpha I} - (r + d)I \right] dt + p_2 \xi_2(t)$$

$$\frac{dR(t)}{dt} = [rI - (\eta + \mu)R] dt + p_3 \xi_3(t)$$

Linearizing above system with the perturbations  $x_1(t), x_2(t)$  and  $x_3(t)$

i.e., using  $S = x_1 + S^*, I = x_2 + I^*$  and  $R = x_3 + R^*$  we get

$$\frac{dx_1(t)}{dt} = -\frac{\beta}{a} x_2 S^* + p_1 \xi_1(t) \quad (12)$$

$$\frac{dx_2(t)}{dt} = \frac{\beta}{a} x_1 I^* + p_2 \xi_2(t)$$

$$\frac{dx_3(t)}{dt} = p_3 \xi_3(t)$$

Applying Fourier transforms both sides and we obtain,

$$p_1 \xi_1(\omega) = i\omega \tilde{x}_1(\omega) + \frac{\beta}{a} S^* \tilde{x}_2(\omega)$$

$$p_2 \xi_2(\omega) = -\frac{\beta}{a} I^* \tilde{x}_1(\omega) + i\omega \tilde{x}_2(\omega)$$

$$p_3 \xi_3(\omega) = i\omega \tilde{x}_3(\omega)$$

The matrix form of above system is given by

$$\bar{\xi}(\omega) = M(\omega) X(\omega)$$

(13)

and denoting the elements of  $M(\omega)$  are  $m_{11}, m_{12}, m_{13}, m_{21}, m_{22}, m_{23}, m_{31}, m_{32}$  &  $m_{33}$  (row wise) then

$$M(\omega) = \begin{bmatrix} m_{11} & m_{12} & m_{13} \\ m_{21} & m_{22} & m_{23} \\ m_{31} & m_{32} & m_{33} \end{bmatrix} \text{ where}$$

$$\bar{\xi}(\omega) = \begin{bmatrix} p_1 \xi_1(t) \\ p_2 \xi_2(t) \\ p_3 \xi_3(t) \end{bmatrix}; X(\omega) = \begin{bmatrix} x_1(\omega) \\ x_2(\omega) \\ x_3(\omega) \end{bmatrix}; m_{11} = i\omega; m_{12} = \frac{\beta}{a} S^*; m_{13} = 0;$$

$$m_{21} = -\frac{\beta}{a} I^*; m_{22} = i\omega; m_{23} = 0; m_{31} = 0; m_{32} = 0; m_{33} = i\omega;$$

Here  $M(\omega)$  is non-singular matrix then inverse of this matrix exist, therefore from (13)

$$X(\omega) = M^{-1}(\omega) \bar{\xi}(\omega) = N(\omega) \bar{\xi}(\omega) \tag{14}$$

$$\text{Where } N(\omega) = \frac{AdjM(\omega)}{|M(\omega)|} = \begin{bmatrix} n_{11} & n_{12} & n_{13} \\ n_{21} & n_{22} & n_{23} \\ n_{31} & n_{32} & n_{33} \end{bmatrix}$$

Now from the spectral density, we define

$$S_g(\omega) d\omega = \lim_{T \rightarrow \infty} \frac{|\overline{g(\omega)}|^2}{T}$$

where  $g(t)$  a random function with is mean zero and  $S_g(\omega)$  represents the variance of the elements of  $g(t)$  within the interval  $[\omega, \omega + d\omega]$ .

The inverse transform of  $S_g(\omega)$  is the auto covariance function is given by

$$C_g(\tau') = \frac{1}{2\pi} \int_{-\infty}^{\infty} S_g(\omega) e^{i\omega\tau'} d\omega$$

and the variance function  $g(t)$  is given by

$$\sigma_g^2 = C_g(0) = \frac{1}{2\pi} \int_{-\infty}^{\infty} S_g d\omega$$

From (14), the mean value of the population is  $\bar{x}_i = \sum_{j=1}^3 n_{ij} \xi_j(\omega)$  where  $b_{ij}, i, j = 1, 2, 3$

$$\text{Therefore, } S_{x_i} = \sum_{j=1}^3 q_j |n_{ij}(\omega)|^2, (i = 1, 2, 3)$$

The fluctuations of  $x_i$  ( $i = 1, 2, 3$ ) are given by

$$\sigma_{x_i}^2 = \frac{1}{2\pi} \int_{-\infty}^{\infty} S_{x_i} d\omega = \frac{1}{2\pi} \sum_{j=1}^3 \int_{-\infty}^{\infty} q_j |n_{ij}(\omega)|^2 d\omega$$

Therefore, from above variances and from system (11), we can find

$$\begin{aligned} \sigma_{x_1}^2 &= \frac{1}{2\pi} \left[ q_1 \int_{-\infty}^{\infty} \left| \frac{A_1}{M(\omega)} \right|^2 d\omega + q_2 \int_{-\infty}^{\infty} \left| \frac{B_1}{M(\omega)} \right|^2 d\omega + q_3 \int_{-\infty}^{\infty} \left| \frac{C_1}{M(\omega)} \right|^2 d\omega \right] \\ \sigma_{x_2}^2 &= \frac{1}{2\pi} \left[ q_1 \int_{-\infty}^{\infty} \left| \frac{A_2}{M(\omega)} \right|^2 d\omega + q_2 \int_{-\infty}^{\infty} \left| \frac{B_2}{M(\omega)} \right|^2 d\omega + q_3 \int_{-\infty}^{\infty} \left| \frac{C_2}{M(\omega)} \right|^2 d\omega \right] \\ \sigma_{x_3}^2 &= \frac{1}{2\pi} \left[ q_1 \int_{-\infty}^{\infty} \left| \frac{A_3}{M(\omega)} \right|^2 d\omega + q_2 \int_{-\infty}^{\infty} \left| \frac{B_3}{M(\omega)} \right|^2 d\omega + q_3 \int_{-\infty}^{\infty} \left| \frac{C_3}{M(\omega)} \right|^2 d\omega \right] \end{aligned} \quad (15)$$

Where  $|M(\omega)| = M_1(\omega) + iM_2(\omega)$  and  $M_1(\omega) = 0$

$$M_2(\omega) = i\omega \left( -\omega^2 + \frac{\beta^2 S^* I^*}{a^2} \right)$$

Where  $|A_1|^2 = \omega^4$ ;  $|B_1|^2 = \left( \frac{\beta}{a} \omega S^* \right)^2$ ;  $|C_1|^2 = 0$ ,  $|A_2|^2 = \left( \frac{\beta}{a} \omega I^* \right)^2$ ;  $|B_2|^2 = \omega^4$ ;  $|C_2|^2 = 0$

$$|A_3|^2 = 0; |B_3|^2 = 0; |C_3|^2 = \left( -\omega^2 + \frac{\beta^2}{a^2} S^* I^* \right)$$

The outcomes in (15) gives the variances of the system (11) populations x and y. For the most part, to discover these integrals it is troublesome. In this manner, by utilizing mathematical reenactments we can clarify these outcomes without any problem. Taking distinctive boundary esteems and for the some delay we can figure difference and this is little then the relating populace is steady, in any case unstable.

## 5 Computer Simulation

Using MATLAB, numerical simulations are given to validate our theoretical results.

**Example 1.** For the model system (1) we explore that the disease free equilibrium exists and is asymptotically stable (left figure in Fig. 2) when the transmission rate  $\beta = 0.1$  along with other parameters value:

$b = 1, a = 3, \alpha = 1, \mu = 0.1, \eta = 0.9, r = 0.81, d = 0.01$  and in this case the basic reproduction rate

$R_0 = 0.41 < 1$ . If the transmission rate  $\beta = 0.9$  and keeping all other parameter values remain same then

endemic equilibrium is exist and is asymptotically stable (right figure in Fig. 2). In this case the basic reproduction rate  $R_0 = 3.66 > 1$ .

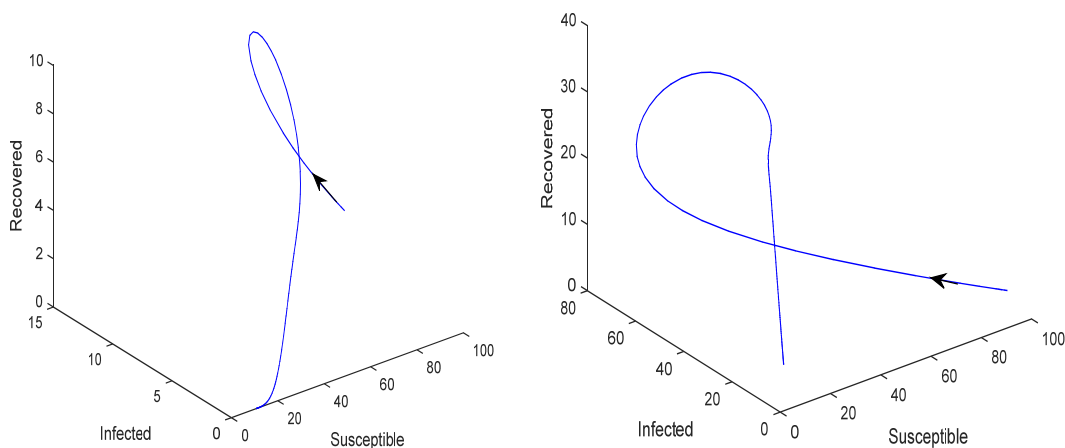


**Fig. 2** Phase portrait of the system (1) with transmission rate  $\beta = 0.1$  (left figure) and  $\beta = 0.9$  (right figure).

**Example 2.** We observe that the endemic equilibrium is initially stable with small incubation period of virus whereas Hopf bifurcation occurs into the system through appearance of limit cycle i.e. endemic equilibrium is unstable for greater value of incubation period.

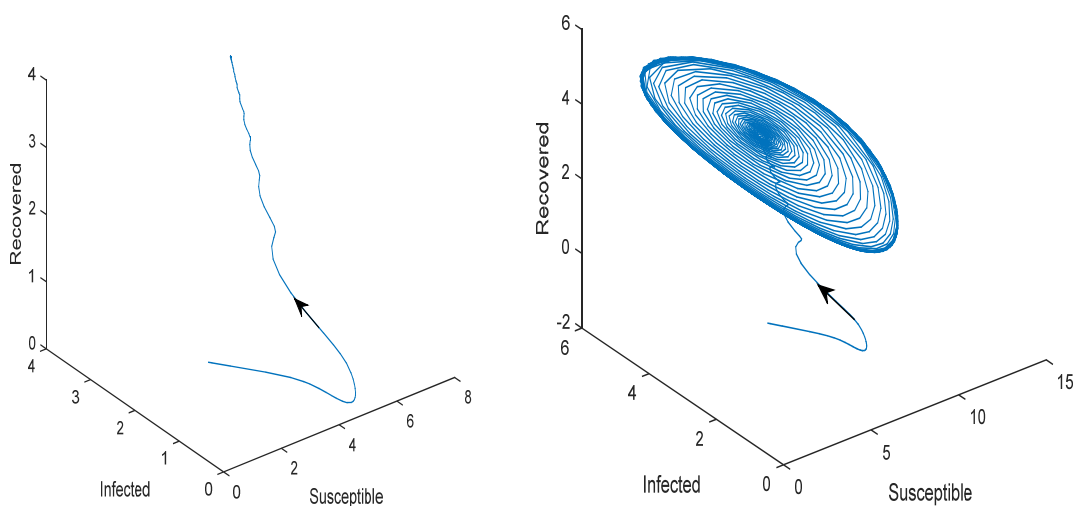


**Fig. 3** Phase portrait of the system (5) with time delay  $\tau = 0.8$  (left figure) and  $\tau = 0.88$  (right figure) with  $b = 1; \beta = 0.9; a = 3; \alpha = 1; \mu = 0.1; \eta = 0.9; r = 0.81; d = 0.01$

**Example 3.** With the high intensities of white noise perturbations we observe that in the model system (11) the endemic equilibrium point ultimately becomes stable although oscillates initially with high amplitude for the parameter values:  $b = 1, a = 3, \alpha = 1, \mu = 0.1, \eta = 0.9, r = 0.81, d = 0.01$ . This indicates that the disease is under controlled with the long run in spite of environmental fluctuations.

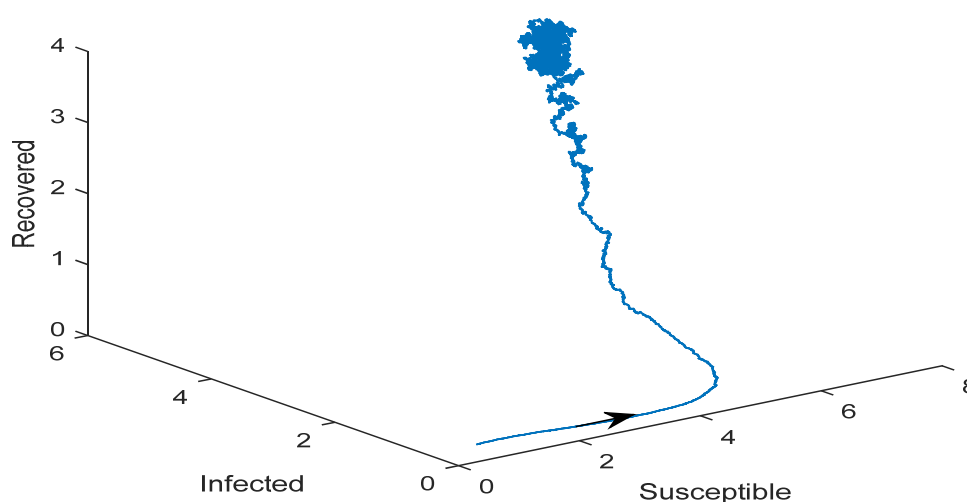


**Fig. 4** Phase portrait of the system (11) with transmission rate  $\beta = 0.9$  and white noises  $\sigma_1 = 0.4, \sigma_2 = 0.7, \sigma_3 = 0.9$ .

## 6 Discussion with Concluding Remarks

We propose a SIRS epidemic model to represent the COVID-19 pandemic in this paper, and we investigate the dynamics of the corona virus under time delay and stochasticity. The model has two equilibrium points: disease free equilibrium and endemic equilibrium, we observe that disease free equilibrium is locally asymptotically stable if  $R_0 < 1$  while endemic equilibrium is locally asymptotically stable if  $R_0 > 1$  (Fig. 2).

The presence of Hopf bifurcation was studied by including a time delay in the transmission terms to represent the virus's incubation period. According to the numerical simulations in Fig. 3, as the virus's incubation period lengthens, periodic outbreaks develop in the system, implying that re-disease and intermittent episodes can occur in the presence of time-delay. Furthermore, by integrating white noise perturbations into the system, we examine the stochastic stability of the system, and our findings reveal that with large white noise intensities, the populations give birth to radically intractable oscillations (Fig. 4). This suggests that white noise is vital in preventing the sickness from spreading.

In summary, the stochastic SIRS model is an attempt to appreciate the epidemiological properties of COVID-19 in this article, and the model analysis provides a few new perspectives into epidemiological situations when natural commotion and time-delay are taken into account.

**Acknowledgments:** The support from Department of Basic and Applied Sciences, NIFTEM and NIFTEM Knowledge Centre is greatly acknowledged.

## References

- Abdo MS, Hanan KS, Satish AW, Pancha K. 2020. On a comprehensive model of the novel coronavirus (COVID-19) under Mittag-Leffler derivative. *Chaos, Solitons and Fractals*, 135: Article ID 109867
- Abdon A. 2017. Fractal-fractional differentiation and integration: connecting fractal calculus and fractional calculus to predict complex system. *Chaos, Solitons and Fractals*, 102: 396-406
- Abdon A. 2018. Blind in a commutative world: simple illustrations with functions and chaotic attractors. *Chaos, Solitons and Fractals*, 114: 347-363
- Abdon A. 2020. Fractional discretization: the African's tortoise walk. *Chaos, Solitons and Fractals*, 130: Article ID 109399
- Bahar A, Mao X. 2004. Stochastic delay Lotka–Volterra model. *Journal of Mathematical Analysis and Applications*, 292: 364-380
- Bocharov G, Rihan FA. 2000. Numerical modelling in biosciences using delay differential equations. *Journal of Computational and Applied Mathematics*, 125: 183-199
- Bogoch II, Watts A, Thomas-Bachli A, Huber C, Kraemer MUG, Khan K. 2020. Pneumonia of unknown aetiology in Wuhan, China: potential for international spread via commercial air travel. *Journal of Travel Medicine*, 27(2): taaa008
- Cakan S. 2020. Dynamic analysis of a mathematical model with health care capacity for COVID-19 pandemic. *Chaos Solitons Fractals*, 139: Article ID 110033
- Dalal N, Greenhalgh D, Mao X. 2008. A stochastic model for internal HIV dynamics. *Journal of Mathematical Analysis and Applications*, 341(2): 1084-1101
- Grifoni A, Weiskopf D, et al. 2020. Targets of T cell responses to SARS-CoV-2 coronavirus in humans with COVID-19 disease and unexposed individuals. *Cell*, 181: 1489-1501
- Hale J. 1977. *Theory of Functional Differential Equations*, Springer-Verlag, New York, USA
- Hui D, et al. 2020. The continuing 2019-ncov epidemic threat of novel coronavirus to global health—the latest 2019 novel coronavirus outbreak in Wuhan, China. *International Journal of Infectious Diseases*, 91: 264-266
- <https://www.who.int/emergencies/diseases/novel-coronavirus-2019/advice-for-public> (2020)
- Ji W, Wang W, Zhao X, Zai J, Li X. 2020. Cross species transmission of the newly identified coronavirus 2019 CoV. *Journal of Medical Virology*, 92(4): 433-440
- Khan MA, Atangana A. 2020. Modeling the dynamics of novel coronavirus (2019-nCov) with fractional derivative. *Alexandria Engineering Journal*, 59(4): 2379-2389
- Kuang Y. 1993. *Delay Differential Equations with Applications in Population Dynamics*. Academic Press, New York, USA
- Lahrouz A, Settati A. 2014. Necessary and sufficient condition for extinction and persistence of SIRS system with random perturbation. *Applied Mathematics and Computation*, 233: 10-19
- Li Q, Guan X, Wu P, et al. 2020. Early transmission dynamics in Wuhan, China, of novel coronavirus-infected pneumonia. *The New England Journal of Medicine*, 382(13): 1199-1207
- Liu Q, Jiang D, Hayat T, Alsaedi A. 2018. Dynamics of a stochastic tuberculosis model with antibiotic resistance. *Chaos Solitons Fractals*, 109: 223-230
- Mao X, Sabanis S, Renshaw E. 2003. Asymptotic behaviour of the stochastic Lotka–Volterra model. *Journal of Mathematical Analysis and Applications*, 287: 141-156
- Mao X, Yuan C, Zou J. 2005. Stochastic differential delay equations of population dynamics. *Journal of Mathematical Analysis and Applications*, 304: 296-320

- Nesteruk I. 2020. Statistics-based predictions of coronavirus epidemic spreading in mainland China. *Innovative Biosystems and Bioengineering*, 4(1): 13-18
- Okhuese VA. 2020. Mathematical predictions for coronavirus as a global pandemic. ResearchGate.
- Ruan S, Wei J. 2003. On the zeros of transcendental functions with applications to stability of delay differential equations with two delays, *Dynamics of Continuous, Discrete and Impulsive Systems Series A*, 10: 863-874
- Shah K, Abdeljawad T, Mahariq I, Jarad F. 2020. Qualitative analysis of a mathematical model in the time of COVID-19. *BioMed Research International*, 2020: Article ID 5098598
- Tornatore E, Vetro P, Buccellato SM. 2014. SIVR epidemic model with stochastic perturbation. *Neural Computing and Applications*, 24(2): 309-315
- Tornatore E, Buccellato SM, Vetro P. 2005. Stability of a stochastic SIR system. *Physica A: Statistical Mechanics and its Applications*, 354(1-4): 111-126
- Ud Din, Shah K, Ahmad I, Abdeljawad T. 2020. Study of transmission dynamics of novel COVID-19 by using mathematical model. *Advances in Difference Equations*, 2020: Article ID 323
- Wei F, Xue R. 2020. Stability and extinction of SEIR epidemic models with generalized nonlinear incidence. *Mathematics and Computers in Simulation*, 170: 1-15
- WHO. 2020. Report of the WHO–China joint mission on coronavirus disease 2019 (COVID-19). World Health Organization, Switzerland
- Xu C, Liao M. 2017. Dynamical behavior for a stochastic two-species competitive model. *Open Math*, 15: 1258-1266
- Xu C, Liao M, Li P, Xiao Q, Yuan S. 2019 A new method to investigate almost periodic solutions for an Nicholson's blowflies model with time-varying delays and a linear harvesting term. *Mathematical Biosciences and Engineering*, 16(5): 3830-3840
- Xu C, Liao M., Li P. 2019a. Bifurcation control of a fractional-order delayed competition and cooperation model of two enterprises. *Science China Technological Sciences*, 62(2): 2130-2143
- Xu C, Li P, Liao M. 2020b. Periodic property and asymptotic behavior for a discrete ratio-dependent food-chain system with delay. *Discrete Dyn. Nature and Society*, 2020: Article ID 9464532
- Yang Q, Mao X. 2013. Extinction and recurrence of multi-group SEIR epidemic models with stochastic perturbations. *Nonlinear Analysis. Real World Applications*, 14: 1434-1456
- Yousaf M, Muhammad SZ, Muhammad RS, Shah HK. 2020. Statistical analysis of forecasting COVID-19 for upcoming month in Pakistan. *Chaos Solitons Fractals*, 138: Article ID 109926.
- Zeb A, Alzahrani E, Erturk VS, Zaman G. 2020. Mathematical model for coronavirus disease 2019 (COVID-19) containing isolation class. *BioMed Research International*, 2020: Article ID 3452402
- Zhao X, Zeng Z. 2019. Stationary distribution and extinction of a stochastic ratio dependent predator prey system with stage structure for the predator. *Physica A: Statistical Mechanics and its Applications*, 545: 1233310
- Zhang WJ, Chen ZL, Lu Y, et al. 2020. A generalized discrete dynamic model for human epidemics. *Computational Ecology and Software*, 10(3): 94-104
- Zhou P, Yang XL, Wang XG, et al. 2020. A pneumonia outbreak associated with a new coronavirus of probable bat origin. *Nature*, 579(7798): 270-273
- Zhu L, Hu H. 2015. A stochastic SIR epidemic model with density dependent birth rate. *Advances in Difference Equations*, 2015: Article ID330